Hindawi
Applied Computational Intelligence and Soft Computing
Volume 2022, Article ID 2117771, 12 pages
https://doi.org/10.1155/2022/2117771

*Research Article*

# Statistical Evaluation and Trend Analysis of ANN Based Satellite Products (PERSIANN) for the Kelani River Basin, Sri Lanka

**Helani Perera,[1] Miyuru B. Gunathilake,[2] Ravindu Panditharathne,[1] Najib Al-mahbashi,[3] and Upaka Rathnayake[1]**

[1]*Department of Civil Engineering, Faculty of Engineering, Sri Lanka Institute of Information Technology, Malabe, Sri Lanka*
[2]*Division of Environment and Natural Resources, Norwegian Institute of Bioeconomy and Research, Ås, Norway*
[3]*Department of Civil and Environmental Engineering, Universiti Teknologi Petronas, Perak 32610, Malaysia*

Correspondence should be addressed to Upaka Rathnayake; upaka.r@sliit.lk

Received 3 June 2022; Revised 4 August 2022; Accepted 17 August 2022; Published 31 August 2022

Academic Editor: V. E. Sathishkumar



Satellite-based precipitation products, (SbPPs) have piqued the interest of a number of researchers as a reliable replacement for observed rainfall data which often have limited time spans and missing days. The SbPPs possess certain uncertainties, thus, they cannot be directly used without comparing against observed rainfall data prior to use. The Kelani river basin is Sri Lanka's fourth longest river and the main source of water for almost 5 million people. Therefore, this research study aims to identify the potential of using SbPPs as a different method to measure rain besides using a rain gauge. Furthermore, the aim of the work is to examine the trends in precipitation products in the Kelani river basin. Three SbPPs, precipitation estimation using remotely sensed information using artificial neural networks (PERSIANN), PERSIANN-cloud classification system (CCS), and PERSIANN-climate data record (CDR) and ground observed rain gauge daily rainfall data at nine locations were used for the analysis. Four continuous evaluation indices, namely, root mean square error (RMSE), (percent bias) PBias, correlation coefficient (CC), and Nash–Sutcliffe efficiency (NSE) were used to determine the accuracy by comparing against observed rainfall data. Four categorical indices including probability of detection (POD), false alarm ratio (FAR), critical success index (CSI), and proportional constant (PC) were used to evaluate the rainfall detection capability of SbPPs. Mann–Kendall test and Sen's slope estimator were used to identifying whether a trend was present while the magnitudes of these were calculated by Sen's slope. PERSIANN-CDR performed well by showing better performance in both POD and CSI. When compared to observed rainfall data, the PERSIANN product had the lowest RMSE value, while all products indicated underestimations. The CC and NSE of all three products with observed rainfall data were also low. Mixed results were obtained for the trend analysis as well. The overall results showed that all three products are not a better choice for the chosen study area.

## 1. Introduction

Rainfall is a crucial component in the hydrological cycle that plays a vital role in water-related activities such as agriculture, hydro-power generation, water resource management, climatology, meteorology, and disaster mitigation [1]. A research study done by Watson and Challinor [2] stated that rainfall is sensitive to the accuracy of models used to simulate crop growth, especially in areas that experience limited rainfall. This marks the importance of precipitation data for hydrological models. Accurate data is important to calibrate and validate hydrological models which will be used for future forecasting for different applications [3]. Therefore, selecting accurate rainfall data as the input is of utmost importance [4].

There are three main types of techniques used in the estimation of rainfall measurements. They are ground-based rain gauge observations, weather radar observations, and satellite data sets [5]. Observed rain gauge data are thought to be the most accurate and dependable source of rainfall data. However, collecting continuous rain gauge data are a difficult task in many parts of the world due to administrative and technical constraints [6]. Due to complex topographical features, installation and maintaining ground-

based rain gauges have been limited [7]. The distribution of rain gauges is limited due to high installation and maintenance costs mainly in developing countries [8]. Therefore, missing data are a huge concern due to these limitations in rain gauge data, [4]. Due to the short length of rainfall records in these rain gauge stations, accurate hydrological modeling with the use of these data will lead to uncertain outcomes [6].

As a solution for the abovementioned limitations and shortcomings identified in rain gauge data, multisatellite high-resolution precipitation products such as tropical rainfall measuring mission (TRMM) multisatellite precipitation analysis (TMPA), precipitation estimation from remotely sensed information using artificial neutral network (PERSIANN) system, multisatellite precipitation analysis, and multisatellite rainfall estimate with climate prediction center (CPM) and morphing technique (CMORPH) and weather radar observations are widely in use around the world [9–11].

SbPPs provide higher spatiotemporal data at no cost [12]. However, these SbPPs are only used after a careful investigation in the desired study area. Since it was discovered that these SbPPs have certain uncertainties, such as accuracy that is affected by topographical features of the study area and precipitation mechanism due to seasonal and regional climate conditions, such accuracy evaluations of the products with respect to rain gauge data are done for each area of concern [7, 9, 10], which cannot be ignored if we plan to use them in hydrological applications [6]. A study done by et al., [13] in the Ganzi river basin of the Tibetan plateau to evaluate the impact of satellite data sets to be used in hydrological modeling for that area used CMORPH-CRT, PERSIANN-CDR, 3B42RT, and 3B42 satellite data sets against observed rainfall data using HEC-HMS model to find out that TRMM-3B42RT and CMORPH-CRT show good performance in the respective area and they also suggested that TRMM-3B42RT is a better choice overall for hydrological models in the Ganzi river basin of Tibetan plateau.

On the other hand, PERSIANN products have been widely applied to many countries. Sorooshian et al. [14] have tested the PERSIANN precipitation products to tropical rainfalls in the United States. Their findings concluded the necessity of further improvement to the SbPPs in the direction of spatial resolutions and accuracy. In addition, Ashouri et al. [15] stated the high applicability of PERSIANN products in various hydrological scenarios. Hurricane Katrina (in 2005) and Sydney flood in Australia (in 1986) were two of the verified cases of higher accuracies from PERSIANN precipitation products. However, Hong et al. [16] stated the overall PERSIANN products are in good agreement with northwestern Mexico rain gauges. Nevertheless, in some of the cases, the PERSIANN underestimated the precipitations. Furthermore, Miao et al. [17] have also ensured the performance of PERSIANN products in eastern China. Therefore, PERSIANN precipitation products can be applied to many other areas after investigating their accuracy over localized regions. Sri Lanka is a country in which the economy mainly depends on agricultural activities. Therefore, the presence of accurate rainfall data for future drought and flood forecasting is essential [18–21]. Even though Sri Lanka has dense rainfall measuring stations (more than 500 for the total area of 65610 $km^2$), some of the stations are scattered in urbanized areas. The remote areas are not uniformly covered by rain gauges. In addition, some of the rain gauges are not properly functioning and regularly maintained due to their remote locations and other logistic issues. Therefore, there can be some disputes in the measured rainfalls even though most of the researchers treated them to be highly accurate.

Thus, it is important to understand the behavior of SbPPs as an alternative input variable for hydrologic and hydraulic studies. However, the spatio-temporal variation of rainfall is highly dynamic from catchment to the catchment. Therefore, the acceptability of a particular SbPP has to be investigated in a localized context.

Despite the fact that several studies have been conducted in many places around the world, no such evaluation of SbPPs using observed rainfall data has been conducted for the Kelani river basin in Sri Lanka, which is the country's fourth longest river [22, 23]. This research study aims to identify the appropriateness of using PERSIANN SbPPs as an alternative to observe rain gauge measurements and also to analyze the trends in both SbPP and rain gauge data in the Kelani river basin, Sri Lanka. As per the authors' best knowledge, this is the first-ever study to investigate the acceptability of any SbPPs against the ground-measured rainfall in the Kelani river basin.

## 2. Study Area and Data Used

*2.1. Study Area.* Sri Lanka is a country having 103 river systems that start from the central mountains and flow down to the coastal areas. Out of those 103 rivers, the Kelani river is the fourth-longest river which originates from the Sri Pada Mountain range (Adam's peak range), and passes through four districts of Nuwara–Eliya, Kegalle, Gampaha, and Colombo in the country and flows down to the Indian Ocean through the Colombo [23]. It is about 145 km long and the basin drains an area of over 2340 $km^2$ being the seventh-largest river basin in Sri Lanka. The Maha Oya and Attanagalu rivers mark the divide between the northeast and northwest boundaries of the watershed [22]. Because it is a river basin in the country's wet zone, the river's average annual discharge is around 4969 million cubic meters (MCM) [24]. During the southwest monsoon season, the Kelani river basin receives the most rainfall, with an average annual precipitation of 2400 mm [7]. The Kelani river is located in a very fertile and populated zone with the elevation varying from sea level to above 2000m above mean sea level (AMSL). The upper catchment is mountainous, whilst the lower catchment is nearly flat [22]. Due to these geographical orientations and the terrain of the basin, the Kelani river basin is very vulnerable to flooding [23]. This basin is of utmost importance to the country as this basin provides hydropower using Castlereagh, Laxapana, and Maussakelle reservoirs in the upper catchment area [23, 25]. The elevation map and the rain gauge stations located in the Kelani river basin are demonstrated in Figure 1.

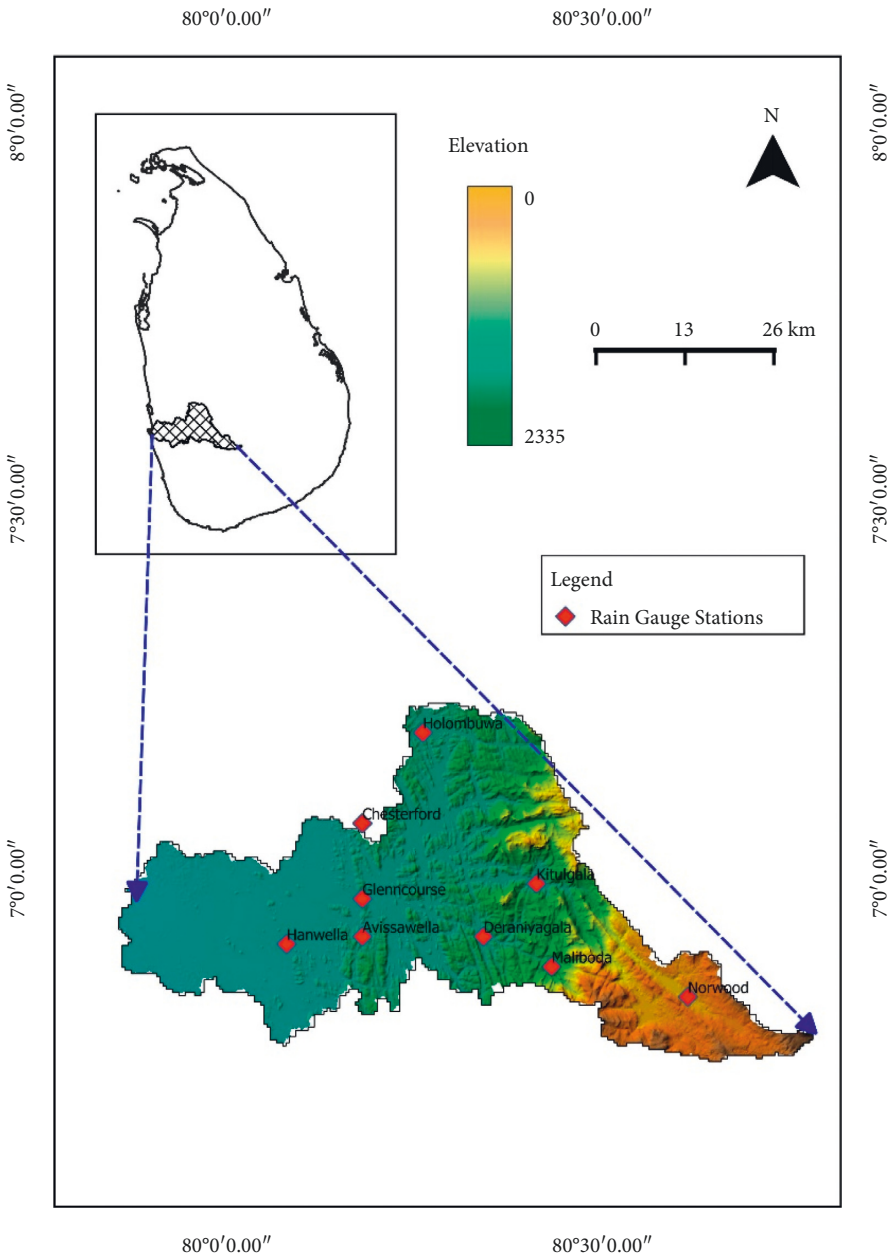


Figure 1: Elevation map of Kelani river basin.

Figure 2 presents the land uses for the Kelani river basin. The upstream of the Kelani river basin is visibly covered by forest regions and tea estates, as seen in the figure. These forests and tea estates are in the central hills. However, toward the lower elevations, rubber plantations are dominant in land use. In addition. The downstream of the Kelani river basin is densely populated and covered by built-up areas.

### 2.2. Datasets

*2.2.1. Rain Gauge Data.* The observed rain gauge data were obtained from Sri Lanka's department of meteorology, which is the country's official authority for meteorological data gathering. The analysis was based on daily data from nine rain gauge stations located throughout the catchment from 1989 to 2016.

*2.2.2. Satellite Rainfall Products.* Three types of SbPPs from the PERSIANN family of products were used for the analysis. Precipitation data for all nine stations mentioned in Table 1 were obtained from these SbPPs. Table 2 contains general information about the SbPPs employed, and Figure 3 graphically depicts the spatial coverage of the nine recorded rainfall stations in each product's appropriate spatial resolution. The three SbPPs used for the study are as follows:

(i) Precipitation estimation from remotely sensed information using artificial neural networks (PERSIANN)

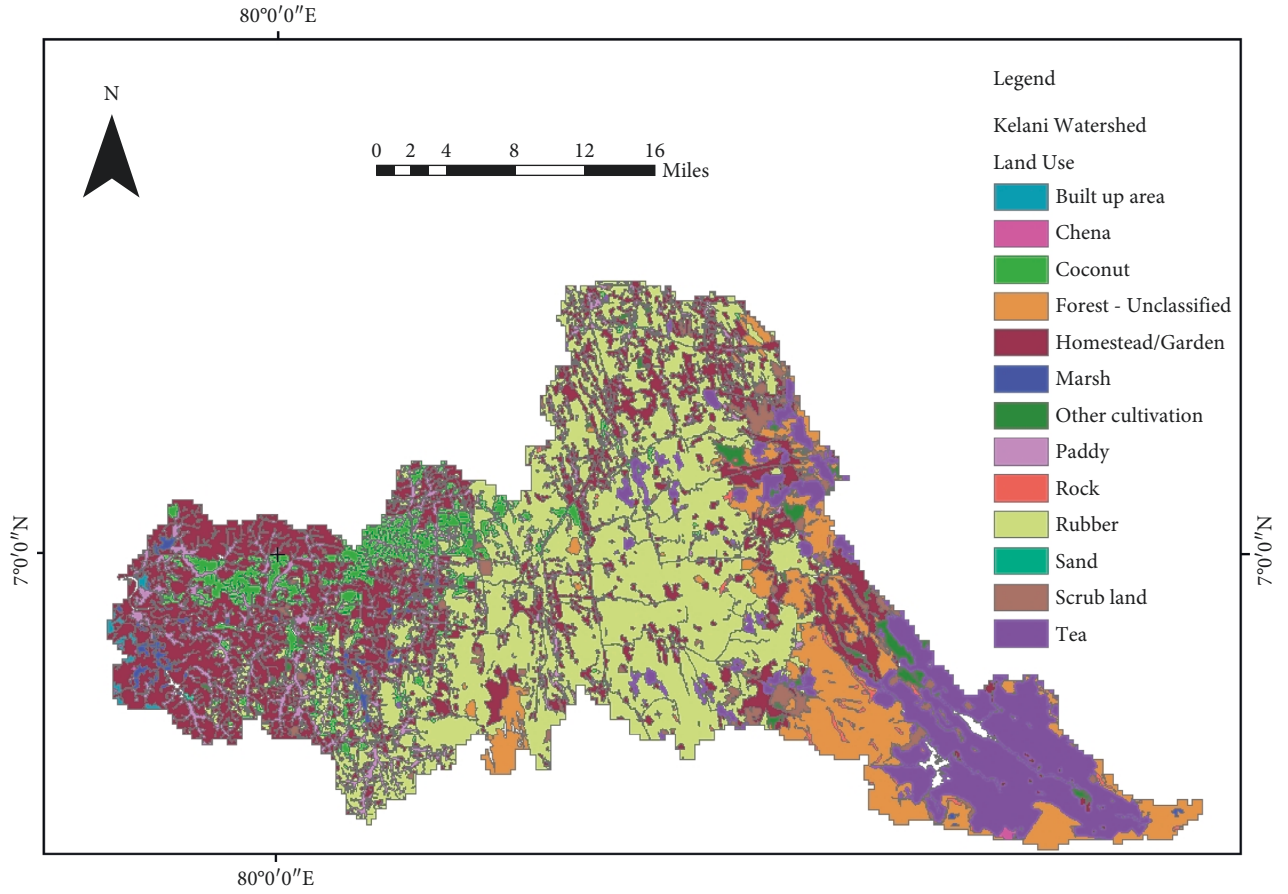


Figure 2: Land use map of Kelani river basin.

Table 1: Details of observed rain gauge stations.

| Station | Latitude (°N) | Longitude (°E) |
|---|---|---|
| Norwood | 6.84 | 80.61 |
| Kitulgala | 6.99 | 80.41 |
| Holombuwa | 7.19 | 80.26 |
| Deraniyagala | 6.92 | 80.34 |
| Glenn course | 6.97 | 80.18 |
| Hanwella | 6.91 | 80.08 |
| Chesterford | 7.07 | 80.18 |
| Maliboda | 6.88 | 80.43 |
| Avissawella | 6.92 | 80.18 |

Table 2: Details of SbPPs.

| SbPPs | Temporal coverage | Finest temporal resolution | Spatial coverage | Spatial resolution |
|---|---|---|---|---|
| PERSIANN | 2000-now | One hour | 60°N to 60°S | 0.25° × 0.25° |
| PERSIANN-CCS | 2003-now | One hour | 60°N to 60°S | 0.04° × 0.04° |
| PERSIANN-CDR | 1983-now | One day | 60°N to 60°S | 0.25° × 0.25° |

(ii) Precipitation estimation from remotely sensed information using artificial neural networks–cloud classification system (PERSIANN–CCS)

(iii) Precipitation estimation from remotely sensed information using artificial neural networks–climate data record (PERSIANN–CDR)

PERSIANN-CDR gets input from the infrared imagery from geostationary (GEO) satellites. It takes the inputs from GEO satellites available since 1979 under a spatial resolution of 10 km. PERSIANN algorithm was developed in 1997 using low Earth orbit (LEO) satellites and high-frequency samples from GEO satellites. The precipitation data can be

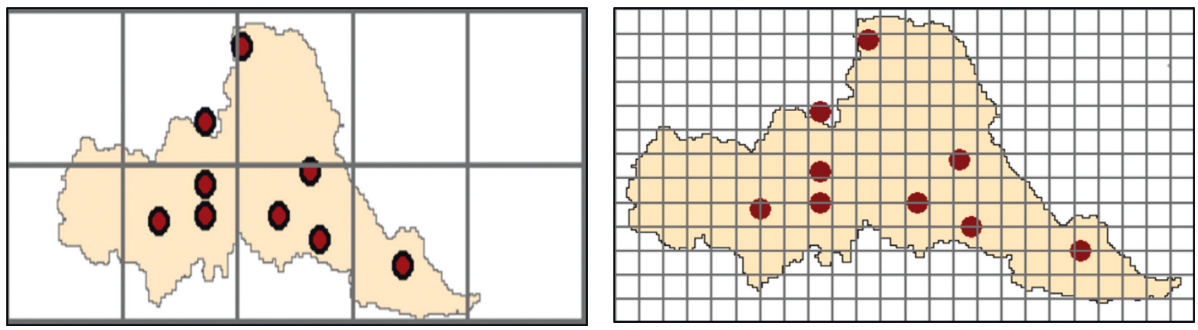

(a) (b)

Figure 3: Spatial distribution of rain gauge stations.

extracted since 2000 for this product. The algorithm was further amended using cloud patch-based algorithms for PERSIANN-CCS. They used specified temperature thresholds. These three SbPPs have differences as listed in Table 2. In addition, PERSIANN-CDR is widely for climate analysis as it covers more than 30 years of data (which can be treated as a climate cycle) whereas the other two SbPPs are widely used for short-term projections.

## 3. Methodology

The accuracy of SbPPs was statistically evaluated using continuous evaluation indicators and categorical indices. Due to the uneven ranges of data availability of three SbPPs (refer to Table 2) and ground-measured rainfall, a common period of 2003–2016 (14 years) was considered for the analysis. In addition, the SbPPs data were extracted directly to the coordinate of the ground-measured rain gauge station. Therefore, the impact of spatial resolution of SbPPs to ground-measured is minimum. Furthermore, nonparametric tests were then used to determine the trends and magnitudes of trends observed in the SbPPs for the area of interest in this study.

*3.1. Continuous Evaluation Indices.* Four continuous indices including root mean square error (RMSE), percentage bias (PBias), coefficient correlation (CC), and Nash–Sutcliffe efficiency (NSE), utilized to assess the effectiveness of SbPPs [21, 25–28]. The RMSE (refer to Equation (1)), PBias (refer to Equation (2)), CC (refer to Equation (3)), NSE (refer to Equation (4)) are given below:

$$\mathrm{RMSE} = \sqrt{\frac{\sum_{i=1}^{n} (S_i - O_i)^2}{n}}, \tag{1}$$

$$P_{\mathrm{bias}} = \left[\frac{\sum_{i=1}^{n} (S_i - O_i)}{\sum_{i=1}^{n} O_i}\right] x\ 100\%, \tag{2}$$

$$\mathrm{CC} = \left[\frac{\sum_{i=1}^{n} (O_i - O_{\mathrm{mean}}) \times (S_i - S_{\mathrm{mean}})}{\sqrt{\sum_{i=1}^{n} (O_i - O_{\mathrm{mean}})^2 \times \sum_{i=1}^{n} (S_i - S_{\mathrm{mean}})^2}}\right]^2, \tag{3}$$

$$\mathrm{NSE} = 1 - \left[\frac{\sum_{i=1}^{n} (S_i - O_i)^2}{\sum_{i=1}^{n} (O_i - O_{\mathrm{mean}})^2}\right], \tag{4}$$

where, $S_i, O_i, n, S_{\mathrm{mean}}$, and, $O_{\mathrm{mean}}$ are estimated precipitation, observed precipitation, number of observations, mean of estimated rainfall data, and mean of observed rainfall data.

*3.2. Categorical Indices.* The SbPPs' prediction and detection abilities were assessed using four categorical indices. Probability of detection (POD), false alarm ratio (FAR), proportion correct (PC), and critical success index (CSI) are the four indices [7, 21–30]. Equations (5) and (6) of the indices are as given below:

$$\mathrm{POD} = \frac{(\mathrm{hits})}{(\mathrm{hits} + \mathrm{misses})}, \tag{5}$$

$$\mathrm{FAR} = \frac{(\mathrm{false\ alarms})}{(\mathrm{hits} + \mathrm{false\ alarm})}, \tag{6}$$

$$\mathrm{PC} = \frac{(\mathrm{hits} + \mathrm{correct\ negatives})}{(\mathrm{hits} + \mathrm{misses} + \mathrm{false\ alarm} + \mathrm{correct\ negatives})}, \tag{7}$$

$$\mathrm{CSI} = \frac{(\mathrm{hits})}{(\mathrm{hits} + \mathrm{misses} + \mathrm{false\ alarm})}. \tag{8}$$

Rainfall intensity class based on their rainfall thresholds, P are described as below [7, 21, 31]:

(i) No/tiny rainfall - $P < 1$ mm
(ii) Light rainfall - $1\ \mathrm{mm} \le P < 2\ \mathrm{mm}$
(iii) Low moderate rainfall - $2\ \mathrm{mm} \le P < 5\ \mathrm{mm}$
(iv) High moderate rainfall - $5\ \mathrm{mm} \le P < 10\ \mathrm{mm}$
(v) Heavy rainfall - $P \ge 10$ mm

For the analysis, 1 mm/day threshold was used which falls under the "light rainfall" intensity class. The contingency table used for the analysis is also given in Table 3 [7, 21].

*3.3. Nonparametric Tests.* The monthly, annual, and seasonal trends of the two datasets were analyzed using the Mann–

Table 3: Contingency table for categorical evaluation indices.

| Event (mm) | Observation event (mm) | |
|---|---|---|
| | Yes ($P \geq 1$) | No ($P < 1$) |
| Yes ($P \geq 1$) | Hits | Misses |
| No ($P < 1$) | Misses | Correct negatives |

Kendall (MK) Test. Sen's slope estimator test was used to determine the magnitude of the trends.

According to the hypothesis used in the Mann–Kendall test $H_0$ indicates that there is no trend in series and $H_1$ indicates there is a trend in series. Mann–Kendall test statistics, $S$ was calculated using the following Equations [32, 33]:

$$S = \sum_{i=1}^{n-1} \sum_{j=i+1}^{n} \operatorname{sgn}\left(y_j - y_i\right)$$

$$\operatorname{sgn}\left(y_j - y_i\right) = \begin{cases} +1, & \text{if } y_j > y_i, \\ 0, & \text{if } y_j = y_i, \\ -1 & \text{if } y_j < y_i, \end{cases} \tag{9}$$

where; $y_j$ and $y_i$ are monthly precipitation values.

The normalized test statistic, $Z_c$ signifies the standard normal distribution and the positive or the negative value of $Z_c$ indicates whether the trend is increasing or decreasing, respectively, [33].

$$Z_c = \begin{cases} \dfrac{S-1}{\sqrt{\operatorname{Var}(S)}}, & S > 0 \\ 0, \quad S = 0 \\ \dfrac{S+1}{\sqrt{\operatorname{Var}(S)}}, & S < 0 \end{cases}, \text{ where } \operatorname{Var}(S) = \frac{n(n-1)(2n+5) - \sum_{i=1}^{t} t_i(i)(i-1)(2i+5)}{18}, \tag{10}$$

where, $n$ is the number of data points, $\mathbf{t}$ is the number of tied groups and $\mathbf{t_i}$ is the number of datasets in the $\mathbf{i^{th}}$ group.

For a normal distribution with a mean of 0 and a standard deviation of 1, the probability density function, $f(z)$, is given by,

$$f(z) = \frac{1}{\sqrt{2\pi}} e^{z^2/2}. \tag{11}$$

If $Z$ is negative and the probability is greater than 0.95, the trend will be found to be decreasing at a 95% significance level. Similarly, if $Z$ is positive and the probability is more than 0.95, the trend will be found to be increasing. If the probability is less than 0.95, it is assumed that there is no trend in the data [34].

Sen's slope is a linear slope estimator used for determining the magnitude of a trend series [35]. The slope of data sets was determined by using Equation (12) and, Sen's slope is given by Equation (13). Positive $Q_i$ values signify increasing trend patterns and, negative $Q_i$ values signify decreasing trend patterns.

$$d_k = \frac{X_j - X_k}{j - i}, \tag{12}$$

where $j > k$, $X$ corresponds to a data value at a $j/k$ time and $k = 1,2, \ldots, N$

$$Q_i = \begin{cases} d_{\frac{(n+1)}{2}}, & n \text{ is odd}, \\ \dfrac{1}{2}\left(d_{n/2} + d_{(n+2/2)}\right), & n \text{ is even}. \end{cases} \tag{13}$$

## 4. Results and Discussion

*4.1. Visual Rainfall Variations.* Figure 4 presents the visual rainfall variations for all stations over the years for observed and SbPPs. Only the annual rainfalls are shown in the figures due to the complexity of the plots. Even though the rainfall from one year to another year is not connected, lines were chosen to develop the plots to showcase the variation of rainfall. Variations can be observed from observed rainfalls to SbPPs and some of these variations are significant. However, the peaks and troughs of SbPPs match the observed rainfalls. In addition, the special features can be seen in Figures 4(e), 4(g), 4(h), and 4(i). The observed rainfall line is not continuous (abnormal in the years 2013 and 2015 to Figure 4(h)). The observed daily rainfalls were unavailable for these years (or for many days) due to instrumental issues and some other logistic issues (like flooding in the area). Therefore, the objective of this research study is clearly stated.

*4.2. Categorical Indices.* Four categorical indices, POD, FAR, CSI, and PC were used to evaluate the rainfall detection capability of each satellite product. POD values for PERSIANN-CCS and PERSIANN-CDR varied in the range of 0.69–0.88. The lowest POD was 0.69 for PERSIANN-CCS and 0.77 for PERSIANN-CDR in Norwood, and the highest was 0.8 for PERSIANN-CCS and 0.88 for PERSIANN-CDR in Glenn course. In the PERSIANN product, the lowest POD value was 0.61 again in Norwood, and the highest value was 0.71 in Avissawella.

For PERSIANN-CCS, the lowest FAR seen was 0.33 in Maliboda, and the highest FAR was seen as 0.45 in Hanwella.

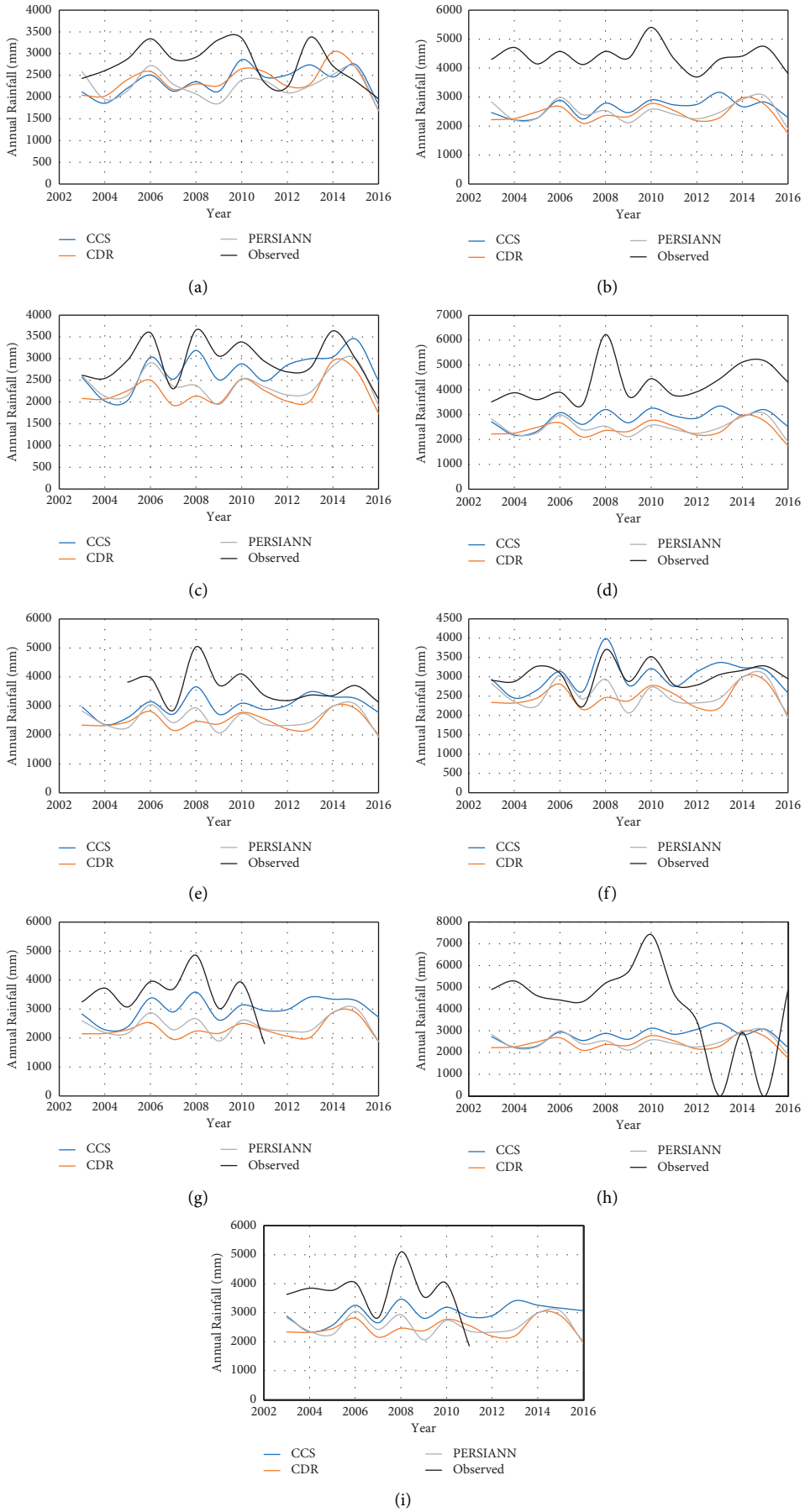


Figure 4: Annual rainfall variations from 2003 to 2016. (a) For Norwood. (b) For Kitulgala. (c) For Holombuwa. (d) For Deraniyagala. (e) For Glenn course. (f) For Hanwella. (g) For Chesterford. (h) For Maliboda. (i) For Avissawella.

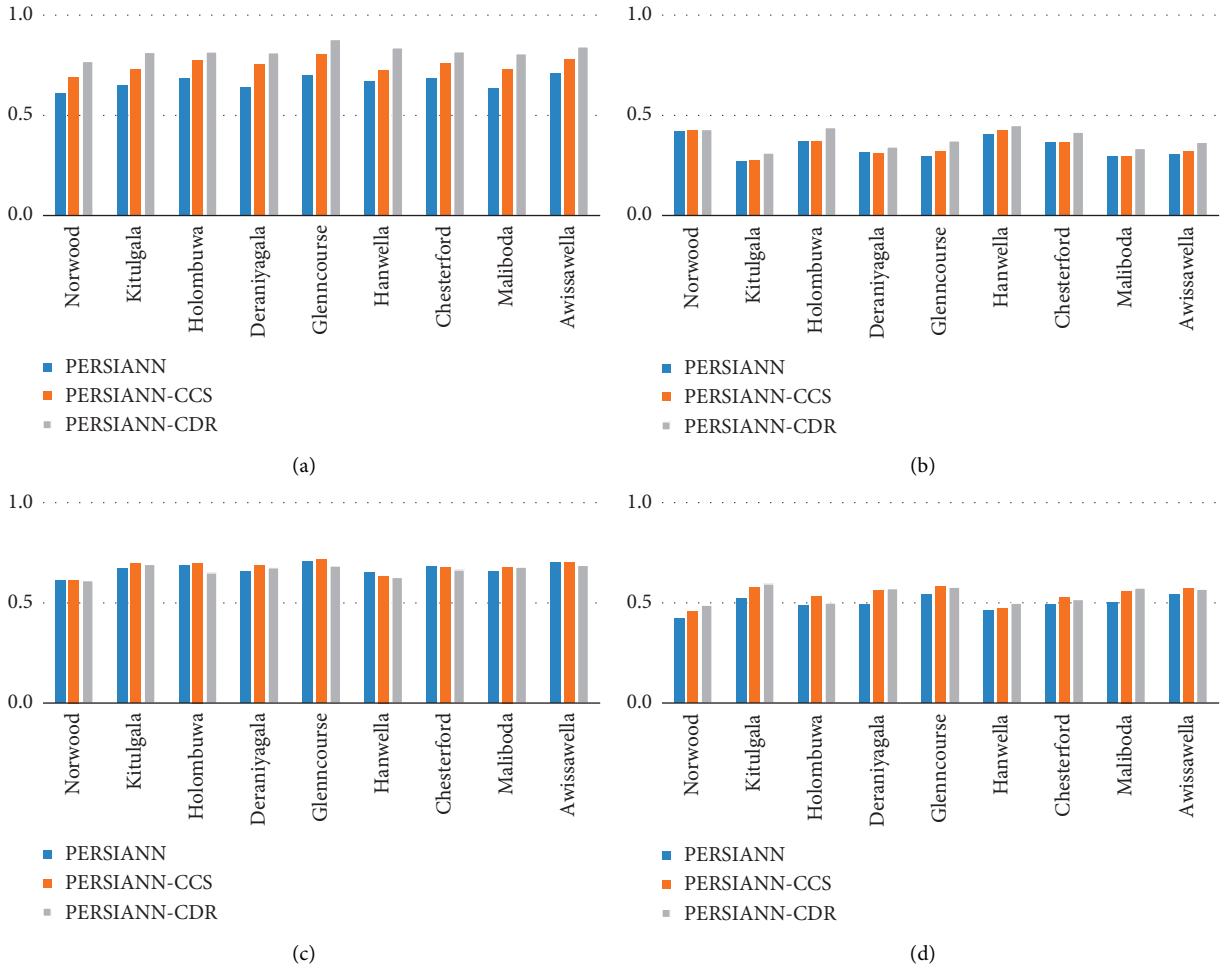


Figure 5: Results of categorical indices. (a) For POD values. (b) For FAR values. (c) For PC values. (d) For CSI values.

For PERSIANN-CDR and PERSIANN products, FAR varied between 0.27–0.43 with the lowest for both products as 0.27 in Kitulgala. Both Norwood and Hanwella stations showed the highest FAR values as 0.43 for PERSIANN-CDR. However, the height FAR value for the PERSIANN product was 0.41 in Hanwella.

PC values for PERSIANN-CCS vary between 0.61 and 0.69, showing the lowest in Norwood and the highest value in Kitulgala. For the PERSIANN-CDR and PERSIANN products, the lowest PC value was 0.61 in Kitulgala, and the highest was 0.71 in Glenn course.

CSI values for PERSIANN-CCS varied between 0.49–0.59 while showing the lowest CSI as 0.49 in Norwood and the highest as 0.59 in Kitulgala. For PERSIANN-CDR, the lowest CSI values were observed as 0.46 in Norwood and the highest as 0.58 in Glenn course. For the PERSIANN product, CSI values ranged from 0.42–0.54 with the lowest in Norwood and highest in both Avissawella and Glenn course stations.

Comparatively, from the stationwise mean values, higher results for accurate rainfall detections (POD) were observed in PERSIANN-CDR (POD > 0.8). PERSIANN product showed high performance in having a lower fraction of false rainfall detections (FAR) compared to other products. PERSIANN-CCS and CDR both indicated good performance in correct rainfall predictions (CSI). Among the three products evaluated for detection and prediction capabilities, PERSIANN-CDR proved to be a better product by showing better performance in both POD and CSI. Similar results can also be seen in a study done in upper Nan river basin, Northern Thailand by Gunathilake et al. [7]. Figure 5 represents the results obtained.

*4.3. Continuous Evaluation Indices Results.* In the PERSIANN-CCS product, RMSE values were in the range of 17–24.5 mm/day, the PERSIANN-CDR product showed RMSE values ranging from 16–22.3 mm/day and the PERSIANN product showed RMSE values in the range of 15.5–22.5 mm/day for all nine stations. In terms of RMSE, better performance was showcased by PERSIANN product by having relatively lower errors.

All stations show negative PBias values which signify underestimation. Stationwise mean values for PERSIANN-CCS was 22.70%, PERSIANN-CDR was 35.29% and PERSIANN was 28.67%. Considering all three types of satellite products, PERSIANN-CCS showed the lowest percentage bias between the observed and satellite datasets while

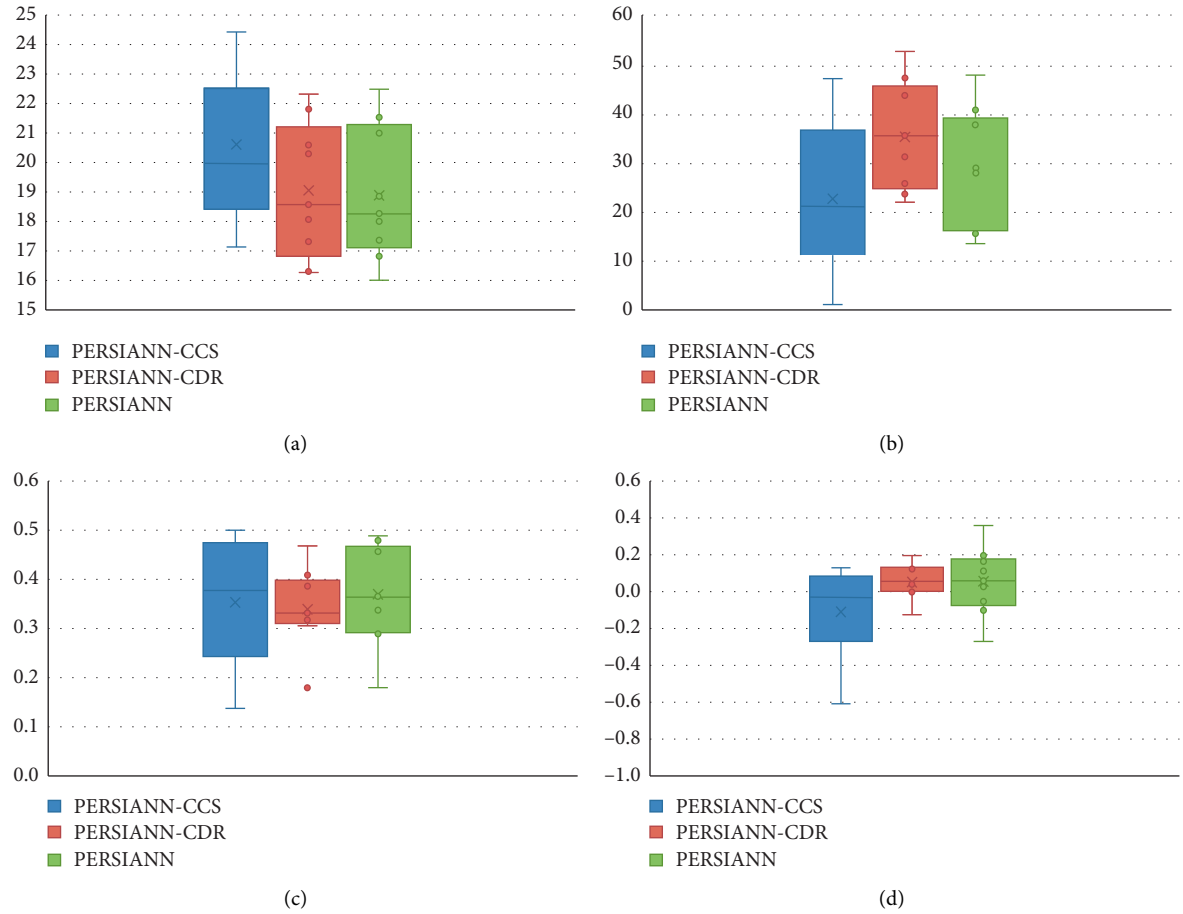


Figure 6: Results of continuous evaluation indices. (a) For RMSE. (b) For PBias. (c) For CC. (d) For NSE.

PERSIANN-CDR showed the highest percentage bias as observed in the results.

CC values for all products in all nine stations varied between 0.14–0.49. The stationwise mean values calculated for each product showed that the correlation between the two datasets with all three satellite products shows not much difference. The correlation is relatively less and falls in the moderate range [30]. However, all products showed positive correlations with the observed data.

Most of the stations produced negative NSE values in the PERSIANN-CCS product which indicates unacceptable performance. However, PERSIANN-CDR and PERSIANN obtained values in the range of 0 and 1 for NSE in most of the stations and thus proved acceptable levels of performance. None of the products showed optimal performance in NSE when compared with the stationwise mean values.

In continuous evaluation indices, the lowest RMSE value was observed in the PERSIANN product which indicated values lower than the stationwise mean value for six out of nine stations [36]. In PBias results, all three satellite data types show underestimation by indicating positive values. Compared to the other two satellite data sets, PERSIANN-CDR shows larger underestimations in all nine stations [36]. CC results for all three products showed values between 0–0.5 which cannot be counted as a significantly good range. NSE also showed values less than 0.5 in all stations for PERSIANN-CCS, PERSIANN-CDR, and PERSIANN which again is not closer to the optimal value of 1 [33]. Among the evaluated three products with continuous evaluation indices, PERSIANN-CDR showed better performance overall followed by the PERSIANN product and PERSIANN-CCS product. Figure 6 represents the results obtained.

*4.4. MK Test and Sens Slope Estimator Results.* Trend analysis using MK test for monthly time scale was done to identify any similar significant positive or negative trends in observed data and satellite data. The trends observed were then quantified using Sen's slope estimator. The annual and seasonal trend analysis of the observed data in all nine stations yielded no significant trends. Similarly, no significant trends were observed in all three products under evaluation as well. However, in the monthly trend analysis, observed data showed a significant decreasing trend in Kitulgala station in the month of July with a magnitude of 7.5 mm/month. Increasing trends were observed in March at Deraniyagala and Avissawella stations. Another increasing trend was also observed at Chesterford station in August with a magnitude of 7.9 mm/month. In PERSIANN-CCS products, significant increasing trends were observed in Kitulgala, Holombuwa, Deraniyagala, Chesterford, and Avissawella stations. In the PERSIANN-CDR product, no significant trends were observed in relation

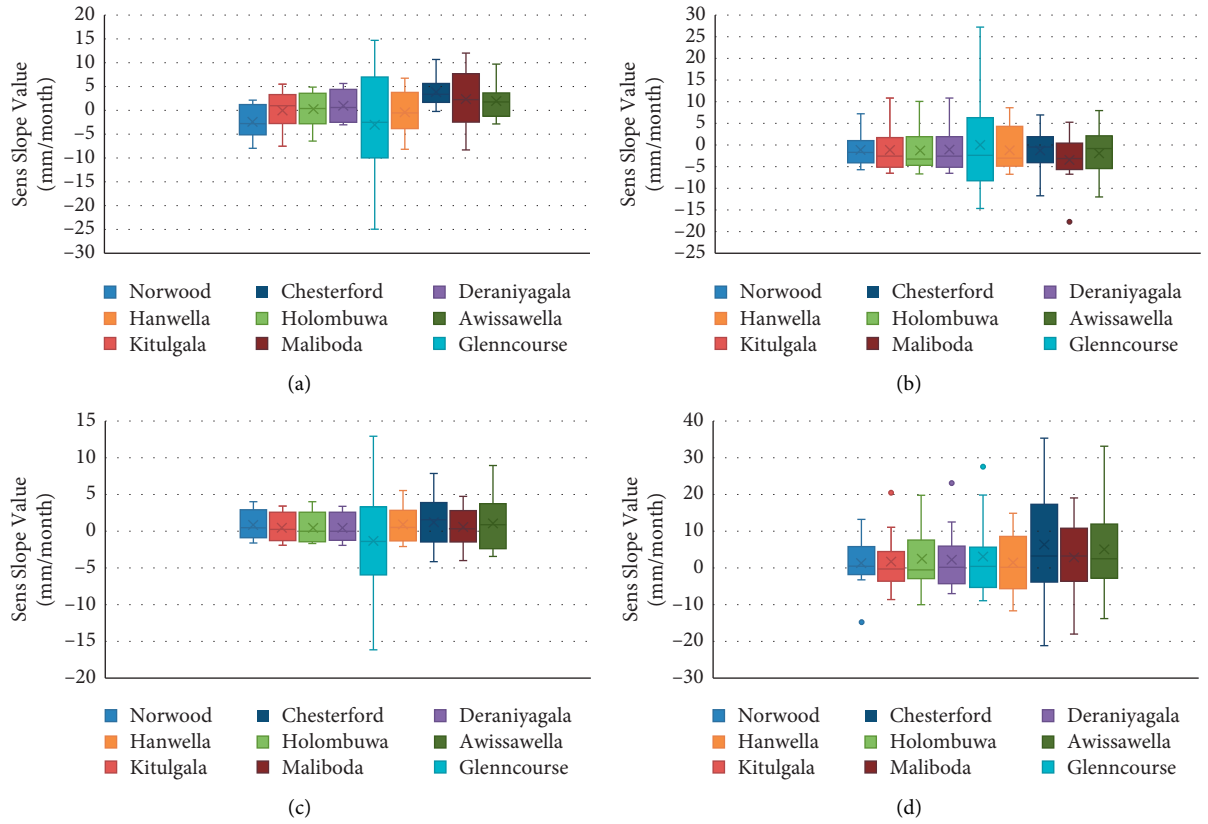


Figure 7: Results of nonparametric test. (a) For observed data. (b) For PERSIANN. (c) For PERSIANN-CDR. (d) For PERSIANN-CSS.

to the trends observed in the observed data. PERSIANN product produced significant trends in Glenn course and Hanwella showed 6.2 mm/month and 4.9 mm/month decreasing trends in January. Kitulgala, Deraniayagala and, Maliboda stations also showed decreasing trends in November with magnitudes of 6.4 mm/month, 6.4 mm/month and, 17.7 mm/month, respectively. PERSIANN-CCS was the only product that showed some relevance in the trends observed with observed data. Figure 7 represents the results obtained.

## 5. Conclusions

This study was carried out in the Kelani river basin, Sri Lanka, to determine the suitability of employing satellite-based precipitation products as an alternative to rain gauge observations and to analyze the trends of each dataset. Three SbPPs, namely, PERSIANN, PERSIANN-CCS, and PERSIANN-CDR were used in this research study. Nine rain gauge stations distributed in the Kelani river basin were used for the analysis. Both observed rainfall data and SbPP data were obtained between the years 1989–2016. Four continuous indices including RMSE, PBias, CC, and NSE, were used to check the accuracy of satellite-based precipitation products by comparing them against observed rainfall. Four categorical indices including POD, FAR, CSI, and PC, were used to evaluate the capability of detection of rainfall in satellite products on a daily scale. MK test was used to identify the trends, and Sen's slope estimator test was used to determine the magnitudes of trends between the two datasets. Results showed that PERSIANN-CDR performed well by showing better performance in both POD and CSI. The lowest RMSE value was observed in the PERSIANN product, and all products showed underestimations when compared with observed rainfall data. The correlation, CC, and NSE of all three products with observed data were also quite weak. Furthermore, from the trend analysis results, few trends were identified in both observed data and satellite data on monthly, annual and seasonal scales however the results were not significant. The results showed that all three products are not a better choice overall for the Kelani river basin, Sri Lanka. Therefore, it is suggested to continue this study with more SbPPs that are readily available to find out the best SbPP alternative for observed rain gauge data in the Kelani river basin, Sri Lanka.

## Data Availability

The climatic data used in this research study are available upon request for research purposes.

## Conflicts of Interest

The authors declare that they have no conflicts of interest.

## Acknowledgments

The authors are grateful to all SRP communities for making the precipitation data freely available to the international research community.

## References


[1] S. Prakash, A. K. Mitra, D. S. Pai, and A. AghaKouchak, "From TRMM to GPM: how well can heavy rainfall be detected from space?" *Advances in Water Resources*, vol. 88, pp. 1–7, 2016.

[2] J. Watson and A. Challinor, "The relative importance of rainfall, temperature and yield data for a regional-scale crop model," *Agricultural and Forest Meteorology*, vol. 170, pp. 47–57, 2013.

[3] M. Collins, K. AchutaRao, K. Ashok et al., "Observational challenges in evaluating climate models," *Nature Climate Change*, vol. 3, no. 11, pp. 940-941, 2013.

[4] Y. Yang, J. Wu, L. Bai, and B. Wang, "Reliability of gridded precipitation products in the yellow river basin, China," *Remote Sensing*, vol. 12, no. 3(374), pp. 1–24, 2020.

[5] H. Li, Y. Hong, P. Xie et al., "Variational merged of hourly gauge-satellite precipitation in China: preliminary results," *Journal of Geophysical Research: Atmospheres*, vol. 120, no. 19, pp. 9897–9915, 2015.

[6] A. Mondal, V. Lakshmi, and H. Hashemi, "Intercomparison of trend analysis of multisatellite monthly precipitation products and gauge measurements for river basins of India," *Journal of Hydrology*, vol. 565, pp. 779–790, 2018.

[7] M. B. Gunathilake, Y. V. Amaratunga, A. Perera, C. Karunanayake, A. S. Gunathilake, and U. Rathnayake, "Statistical evaluation and hydrologic simulation capacity of different satellite-based precipitation products (SbPPs) in the Upper Nan River Basin, Northern Thailand," *Journal of Hydrology: Regional Studies*, vol. 32, p. 100743, 2020.

[8] V. Lakshmi, J. Fayne, and J. Bolten, "A comparative study of available water in the major river basins of the world," *Journal of Hydrology*, vol. 567, pp. 510–532, 2018.

[9] M. M. Bitew and M. Gebremichael, "Evaluation of satellite rainfall products through hydrologic simulation in a fully distributed hydrologic model," *Water Resources Research*, vol. 47, no. 6, pp. 1–11, 2011.

[10] E. Anagnostou, V. Maggioni, E. Nikolopoulos, T. Meskele, F. Hossain, and A. Papadopoulos, "Benchmarking high-resolution global satellite rainfall products to radar and rain-gauge rainfall estimates," *IEEE Transactions on Geoscience and Remote Sensing*, vol. 48, no. 4, pp. 1667–1683, 2010.

[11] G. Villarini, P. V. Mandapaka, W. F. Krajewski, and R. J. Moore, "Rainfall and sampling uncertainties: a rain gauge perspective," *Journal of Geophysical Research*, vol. 113, no. D11, p. D11102, 2008.

[12] D. Kneis, C. Chatterjee, and R. Singh, "Evaluation of TRMM rainfall estimates over a large Indian river basin (Mahanadi)," *Hydrology and Earth System Sciences*, vol. 18, no. 7, pp. 2493–2502, 2014.

[13] A. A. Alazzy, H. Lu, R. Chen, A. B. Ali, Y. Zhu, and J. Su, "Evaluation of satellite precipitation products and their potential influence on hydrological modeling over the Ganzi River Basin of the Tibetan plateau," *Advances in Meteorology*, vol. 2017, pp. 1–23, Article ID 3695285, 2017.

[14] S. Sorooshian, K. L. Hsu, X. Gao, H. V. Gupta, B. Imam, and D. Braithwaite, "Evaluation of PERSIANN system satellite–based estimates of tropical rainfall," *Bulletin Of The American Meteorological Society*, vol. 81, no. 9, pp. 2035–2046, 2000.

[15] H. Ashouri, K. L. Hsu, S. Sorooshian et al., "PERSIANN-CDR: daily precipitation climate data record from multisatellite observations for hydrological and climate studies," *Bulletin of the American Meteorological Society*, vol. 96, no. 1, pp. 69–83, 2015.

[16] Y. Hong, D. Gochis, J. t. Cheng, K. l. Hsu, and S. Sorooshian, "Evaluation of PERSIANN-CCS rainfall measurement using the NAME event rain gauge Network," *Journal of Hydrometeorology*, vol. 8, no. 3, pp. 469–482, 2007.

[17] C. Miao, H. Ashouri, K. L. Hsu, S. Sorooshian, and Q. Duan, "Evaluation of the PERSIANN-CDR daily rainfall estimates in capturing the behavior of extreme precipitation events over China," *Journal of Hydrometeorology*, vol. 16, no. 3, pp. 1387–1396, 2015.

[18] N. Alahacoon and M. Edirisinghe, "Spatial variability of rainfall trends in Sri Lanka from 1989 to 2019 as an indication of climate change," *ISPRS International Journal of Geo-Information*, vol. 10, no. 2, p. 84, 2021.

[19] K. D. W. Nandalal, "Use of a hydrodynamic model to forecast floods of Kalu River in Sri Lanka," *Journal of Flood Risk Management*, vol. 2, no. 3, pp. 151–158, 2009.

[20] S. C. Sugeeswara and A. W. Jayawardana, "Development of a flood forecasting model for kalu river and Kelani River basins in Sri Lanka using radial basis function neural Networks," pp. 1–6, 2010, http://www.icharm.pwri.go.jp/training/master/pubilication/pdf/2010/sugeeswara.pdf.

[21] H. Perera, S. Fernando, M. B. Gunathilake, T. A. J. G. Sirisena, and U. Rathnayake, "Evaluation of satellite rainfall products over the mahaweli river basin in Sri Lanka," *Advances in Meteorology*, vol. 2022, pp. 1–20, Article ID 1926854, 2022.

[22] E. I. L. Silva, R. A. S. N. Jayawardhana, N. P. P. Liyanage, and E. N. S. Silva, "Effects of construction and operation of mini hydropower plants on fish fauna endemic to Sri Lanka-A case study on Kelani River basin," in *Proceedings of the Water Professionals' Day Symposium in Sri Lanka*, vol. 1, Peradeniya, Sri Lanka, October, 2015.

[23] K. D. C. R. Dissanayaka, "Climate extremes and precipitation trends in Kelani river basin, Sri Lanka and impact on streamflow variability under climate change (Doctoral dissertation)," University of Moratuwa, Sri Lanka, India, 2017.

[24] I. D. Hydrological Annual, "Irrigation department, Punjab," 2018, https://irrigation.punjab.gov.pk/.

[25] M. M. G. T. De Silva, S. B. Weerakoon, and S. Herath, "Modeling of event and continuous flow hydrographs with HEC–HMS: case study in the Kelani River Basin, Sri Lanka," *Journal of Hydrologic Engineering*, vol. 19, no. 4, pp. 800–806, 2014.

[26] M. N. Anjum, Y. Ding, D. Shangguan, M. W. Ijaz, and S. Zhang, "Evaluation of high-resolution satellite-based real-time and post-real-time precipitation estimates during 2010 extreme flood event in Swat River Basin, Hindukush region," *Advances in Meteorology*, vol. 2016, pp. 1–8, Article ID 2604980, 2016.

[27] G. Wei, H. Lü, W. T Crow, Y. Zhu, J. Wang, and J. Su, "Evaluation of satellite-based precipitation products from IMERG V04A and V03D, CMORPH and TMPA with gauged rainfall in three climatologic zones in China," *Remote Sensing*, vol. 10, no. 2, p. 30, 2017.

[28] F. Chen and X. Li, "Evaluation of IMERG and TRMM 3B43 monthly precipitation products over mainland China," *Remote Sensing*, vol. 8, no. 6, p. 472, 2016.

[29] M. M. Bitew, M. Gebremichael, L. T. Ghebremichael, and Y. A. Bayissa, "Evaluation of high-resolution satellite rainfall products through streamflow simulation in a hydrological modeling of a small mountainous watershed in Ethiopia," *Journal of Hydrometeorology*, vol. 13, no. 1, pp. 338–350, 2012.

[30] H. Akoglu, "User's guide to correlation coefficients," *Turkish journal of emergency medicine*, vol. 18, no. 3, pp. 91–93, 2018.

[31] M. S. Nashwan, S. Shahid, and X. Wang, "Assessment of satellite-based precipitation measurement products over the hot desert climate of Egypt," *Remote Sensing*, vol. 11, no. 5, p. 555, 2019.
[32] H. B. Mann, "Nonparametric tests against trend. Econometrica," *Journal of the Econometric Society*, vol. 13, pp. 245–259, 1945.
[33] M. G. Kendall, "Rank correlation methods," (4th ed.). Griffin, London, UK, 1948.
[34] P. Khambhammettu, "Mann-kendall analysis, Hydro-GeoLogic inc. OU-1 annual groundwater monitoring report–former fort ord," California, USA, 2005.
[35] S. I. Sridhar and A. Raviraj, "Statistical trend analysis of rainfall in Amaravathi river basin using Mann-Kendall test," *Current World Environment*, vol. 12, no. 1, pp. 89–96, 2017.
[36] P. Nguyen, M. Ombadi, S. Sorooshian et al., "The PERSIANN family of global satellite precipitation data: a review and evaluation of products," *Hydrology and Earth System Sciences*, vol. 22, no. 11, pp. 5801–5816, 2018.